

GeMS sees star light

François Rigaut^{1,a}, Benoit Neichel¹, Céline Dorgeville¹, Damien Gratadour², Maxime Boccas¹, Gelys Trancho³, Matthieu Bec³, Chad Trujillo¹, Michelle Edwards¹, and Rodrigo Carrasco¹

¹ Gemini Observatory, c/o AURA, Casilla 603 La Serena, Chile

² Observatoire de Paris-Meudon, 2 Place Jules Janssen 92195 Meudon-CEDEX France

³ GMTO Corporation - P.O. Box 90933 - Pasadena, CA 91109-0933

Abstract. After a year of commissioning, GeMS/GSAOI, the Gemini MCAO system and its NIR imager, obtained the first compensated images in December 2011. H band Strehl ratios in excess of 35% and FWHMs of or below 50 mas were obtained, in good seeing condition, averaged over the GSAOI field of view of 85x85 arcsec, with an excellent uniformity.

1 Introduction

GeMS is the Gemini Multi-conjugate adaptive optics System. It has been described in more details elsewhere [1–4]. GeMS is currently undergoing its final commissioning phases at the Gemini South telescope. The main components of GeMS are listed below. Note that CANOPUS, that will be used extensively in this paper, is the AO-part/subsystem of GeMS.

- A 50W laser, split into 5 x 10W beams placed on the sky at the corners and center of a 1' square;
- Five Laser Guide Star (LGS) Shack-Hartmann Wave-Front Sensors (WFS), 16x16 subapertures each;
- Three Deformable Mirrors (DM) –currently 2, see text– totalling 917 actuators (684 active, 233 extrapolated), conjugated optically to 0, 4.5 and 9 km above the telescope;
- Three Avalanche PhotoDiodes (APD) based quad-cell Natural Guide Star (NGS) Tip-Tilt (TT) WFS;
- a NGS slow focus WFS (Slow-Focus Sensor–SFS);
- a high order loop running at up to 800 Hz, using a simple leaky integrator law. Approximately 20 more loops or offloads, which make for interesting and challenging calibration schemes;
- Two dedicated instruments:
 - GSAOI (4k2 NIR imager), 85 arcsec Field of View (20 mas pixels) [7]
 - Flamingo II (NIR MOS), 2 arcmin Field of View
- Many subsystems: All-Sky-Camera, Safety systems, infrastructure, laser, Beam Transfer Optics (BTO), Laser Launch Telescope (LLT), etc, that are not described here. Suffice to say that a MCAO system is more than just the AO optical bench. All these "side" subsystems represent more than half the cost and the workload.

Top level specifications included a Strehl ratio of 40% in H band under median seeing conditions (20% in J and 60% in K), a 30% sky coverage (implying a *limiting* magnitude ≥ 18 in R band for TT sensing).

In this paper, we will concentrate on some notable results from the commissioning: initial images and performance of course, but also considerations on Rayleigh scattering, Non common path aberrations (NCPA) and various other aspects. We will also give a top level status of most GeMS components and will briefly talk about lessons learned.

^a e-mail: frigaut@gemini.edu

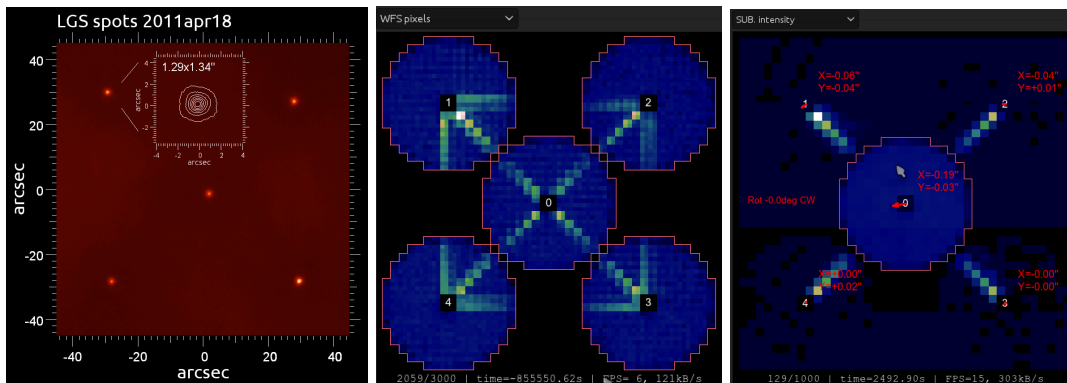


Fig. 1. Left: The 5 spot constellation as seen by the 8-m telescope visible acquisition camera. The 8-m telescope has been focused to about 90km and the Laser Launch Telescope focus has been scanned to get the tightest spots. **center:** LGS WFS subaperture intensity map under normal conditions, showing the Rayleigh pattern in each WFS. Each of the LGS WFS sees four other beams. Note that the beam going to the central LGS and the opposite corner LGS are superimposed in each of the corner WFS. **Right:** Subaperture intensity map seen by the 5 LGS WFSs when only the central beam is propagated. The central WFS (0) sees no Rayleigh. Each of the other WFSs -the ones looking 42 arcsec off axis- see the Rayleigh from the central beam.

2 Commissioning Status and Results

The first phase of commissioning was spread over more than a year. The first commissioning run, 5 nights long, occurred in early January 2011. This was followed by 4 more runs during the first semester of 2011, for a total of 31 nights (out of which only about 20 were clear enough for laser propagation). Early June, as winter got closer, GeMS entered a planned 5 months shutdown period to fix, upgrade and refurbish some of the CANOPUS and the BTO subsystems. Commissioning resumed as planned in November, and proceeded since then with one run a month at the time of this writing (March 2012).

The 2011A commissioning focused on CANOPUS functionalities and LGS facility. Focus shifted toward CANOPUS performance during 2011B, and is gradually transitioning to operation and science in 2012.

2.1 Laser, LGSF and Rayleigh

The first three commissioning runs were mostly dedicated to the laser guide star facility (LGSF). As commissioning progressed, problems were solved and optimization were done, the full 8-m telescope aperture LGS spot FWHM went from 7 arcsec (January, first run), to 3.5 arcsec (second run) and then finally reached a floor of 1.3 arcsec (third run and on). Figure 1 shows an image acquired with the 8-m telescope defocused close to 90km; the spots are about 1.3 arcsec, and are approximately gaussian in shape. More detailed analysis using lucky imaging on very short exposure and working out the full 8-m telescope aperture geometric kernel lead to an intrinsic LGS spot quality of $1.05''$. During 2011, the sodium laser typically outputs 40 to 55 watts at the start of the runs, down by a few to up to 10 watts after one week of continuous operation. Because of the variations of the Sodium content in the Sodium layer, the photon return varied with the season from about 5 to 10 photons/s/cm²/W. We have estimated that 10 photons/s/cm²/W, for a typical laser output power of 45 W, is the threshold to be able to work at 800Hz with the CANOPUS high order loop (see below).

More details can be found in a companion paper [4], which also presents a detailed analysis of the Rayleigh; Why it is not possible to calibrate out with the current instrument capabilities, and the relatively small impact of this effect. But Rayleigh does not only have drawbacks. It has also some benefits which are illustrated below.

To introduce the discussion, it is useful to understand what is actually seen by the LGS WFSs. Figure 1, center panel, gives an example of a "normal" Rayleigh pattern seen by the 5 LGS WFSs.

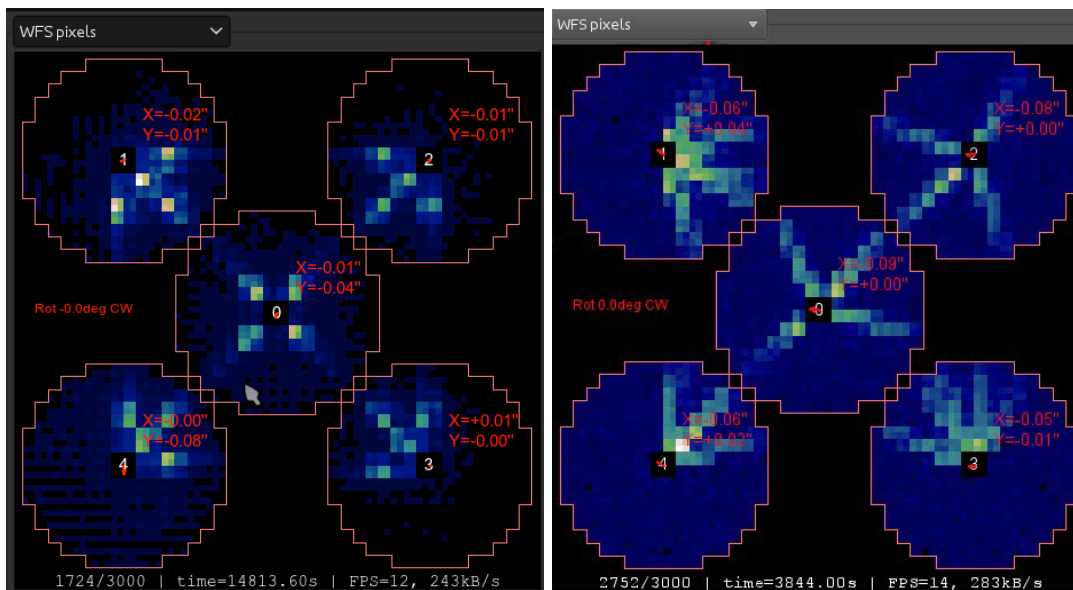


Fig. 2. **Left:** The 5 beam constellation is an excellent cloud detector, here showing a thin layer of cirrus above site. The cloud altitude could be easily retrieved from the location of the bright spots along the Rayleigh pattern. On each corner WFS, the double spot is expected along the beam that points toward the center as there is actually 2 beams superimposed; the one to the center LGS and the one to the opposite corner LGS. **Right:** An example of the subaperture intensity maps seen on the 5 LGS WFSs when the constellation is misaligned, for instance after initial propagation after a slew. This is to be compared with the Rayleigh pattern for best alignment – see figure 1. These patterns are fitted and used for quick re-centering and acquisition. In this example, the constellation pointing is (10",16") off.

To complete this figure and illustrate the explanation, the right panel of figure 1 shows the Rayleigh pattern when only the central beam (central LGS) is on: The central LGS WFS sees a star, but not its own Rayleigh, while each corner LGS WFS sees no star but sees the Rayleigh/fratricide from the central LGS. The "normal" Rayleigh pattern mentioned above (figure 1 center) is a straight extension of this particular case to five beams.

The first "fringe" benefit of Rayleigh is that it constitutes a very sensitive cloud detector, as illustrated in figure 2, left panel. Second, Rayleigh has an important side effect –which was only realized at commissioning time–, which is the ability to greatly accelerate the LGS acquisition by the LGS WFS. The latter has proven to be a significant source of overhead in many LGS AO systems. With GeMS, due to some errors in the BTO pointing optics, or badly compensated flexures, the initial LGS WFS subaperture intensity maps may present as in Fig2, right panel. A simple geometric model of the Rayleigh backscattering has been implemented and a minimization routines provide in a few seconds the geometric solution, out of which the global de-pointing is the most important set of parameters. Once determined, this global de-pointing is applied to the BTO pointing mirrors to re-center the LGS constellation. Once the laser has been propagated and the light sent to CANOPUS, the LGS acquisition thus takes typically less than a minute.

2.2 CANOPUS

At the time of writing, here is a summary of the status of the various bits and ends of GeMS, with an emphasis on CANOPUS, the AO bench and control (also see [4]):

- The main loop, the LGS high order loop, is stable. Our baseline is to use MMSE reconstructors, but MVR reconstructors (provided by Brent Ellerbroek during his visit in April 2011) also work well. LSE reconstructors have been used with success, although they tend naturally to be more

demanding in SNR. With MMSE, we have worked down to 80 photons/subaperture/frame with a stable loop (that is 20 ph/pixel/frame, there are 2x2 pixels/subaperture, the RON is 3.5 e-/pixel), although we generally work at about 150 ph/subaperture/frame, and thus adjust the sampling frequency accordingly. In low Sodium content season (January & February), we generally have to work at 200 frames/s; in medium Sodium content season, at 400 frames/s and in high sodium content season (from April to September) at 400 to 800 frames/s.

- Following the failure of actuators (see [5,4]), we are now working with 2 DMs only, conjugated at 0 and 9 km above site. This means less than half of the actuators originally planned are now used. This somewhat degrades the performance (in average by about 5%, up to 15% in unfavorable conditions) and makes GeMS more sensitive to variation of the Cn2 profile, but on the other hand makes the control more robust (less invisible/degenerate modes). A spare DM is in order and should be received in 2013.
- The TT WFSs have been partially refurbished and part of the throughput loss has been regained. A full analysis is still in progress¹, but it appears there is still close to a 1 magnitude loss compared to e.g. Altair, which uses a TT WFS with a similar APD quad-cell concept (although different in its implementation, as Altair does not use fibers but a STRAP unit that feed directly the light from a focal plane lenslet array to the APDs themselves). We have determined that a large fraction of the loss in the CANOPUS TT WFS is at the fiber injection. Beside the optical throughput limitations, the TT loop is working well, with a maximum sampling rate of 800Hz for a 0dB bandwidth of about 55 Hz. To extract the TT and plate scale modes from the 3 TT WFS signals, we use a MMSE scheme -as for the LGS loop. Kalman and H-infinity loop controllers were also tested [9].
- The plate scale compensation loop is working well and is stable. In particular, the three TT WFS are actually mounted on a common mechanical platform, used for global dithers/offsets. After the setup on an object, the individual TT WFS are held in place on the common platform. This scheme makes for stable and drift-less operation (in the sense of plate scale modes drift), as seen on sky during continuous operation for up to two continuous hours. We have sometimes noticed the gradual apparition of a rotation term, which would need to be compensated by controlling the telescope Cassegrain rotator; Although provisions were made for this since the CANOPUS design phase, it is still to be implemented.
- Most of the BTO Look Up Tables (LUT) are basically working to an acceptable level: the BTO can track a target for hours, although manual re-alignment is necessary once in a while.
- The LGS WFS TT offload to the BTO-Fast Steering Array is working well. It uses the Tip/Tilt signal from each of the LGS WFS to keep the laser spots centered. It runs at 200 Hz.
- The LGS WFS subaperture centroid gains (each subaperture uses 2x2 pixels thus needs a centroid gain to convert from quad-cell signal to arcsec) was originally measured using the BTO FSA to induce the spot dithering in each LGS WFS. This had several issues that are thought to be linked with instabilities in the FSA and/or the FSA hitting some mechanical limits, biasing the input dithering signal and thus the centroid gain estimates. The method has been upgraded to use what we call –wrongly– a ”derviche mode”: this mode is created by the DM0, applying sine and cosine deformations at the cut-off spatial frequency of the DM, with a 1/4 period temporal phase shift between the sine and cosine spatial component. In effect, this makes half the spots turn clockwise and every other spots turn anti-clockwise. This mode has a very low power in the atmosphere, and tip-tilt can be projected out, thus the noise level is very low and a lock-in detection only need a very small power injected into the system to perform an effective detection. Another obvious advantage is that the mode is injected in a component which is common to all LGS WFS, thus preventing any differential estimation error, which is very damaging to the tomographic reconstruction process. An obvious drawback is that this is also common to the science path, thus is seen in the images. However, we proved that 20 nm rms is enough to perform an adequate estimation, thus the impact on Strehl is very minimal, and the effect on the image are predictable satellites in each PSF.

¹ Preliminary results with the upgraded APD units and the refurbished TTWFS1 indicate a detection of 50 photons (total) for a R=15.3 star at 300 Hz

- Tip/Tilt/Focus is offloaded at 200 Hz to M2 (the focus with a very low gain). Six higher order modes (astigmatism, coma and trefoil) are offloaded to M1 once every 30 seconds. These offloads are quite important because of the limited range of the DMs and the TTM.
- On-Detectors-Guide-Windows (ODGW) on GSAOI are basically operational. The flexure loop to stabilize the image long-term on GSAOI has been tested successfully. The fast ODGW guiding still has to be tested.
- The Slow Focus Sensor (SFS) is in the final phases of test and has been used several times during the February 2012 run.

In summary, the vast majority of CANOPUS subsystems –with the notable exception of the ODGW fast guiding– have been commissioned.

The Sodium return has been and is still lower than anticipated originally, mostly because of a lower laser power (and/or lower coupling to sodium atoms) and some throughput loss. In addition, the optical throughput of the CANOPUS TTWFS has been improved but still falls short of the specifications. Upgrades are not completed yet, and may further improve the numbers. Re-designs are being considered to solve this issue. Apart from these shortcomings, the instrument is working to specifications (see below for some preliminary performance numbers).

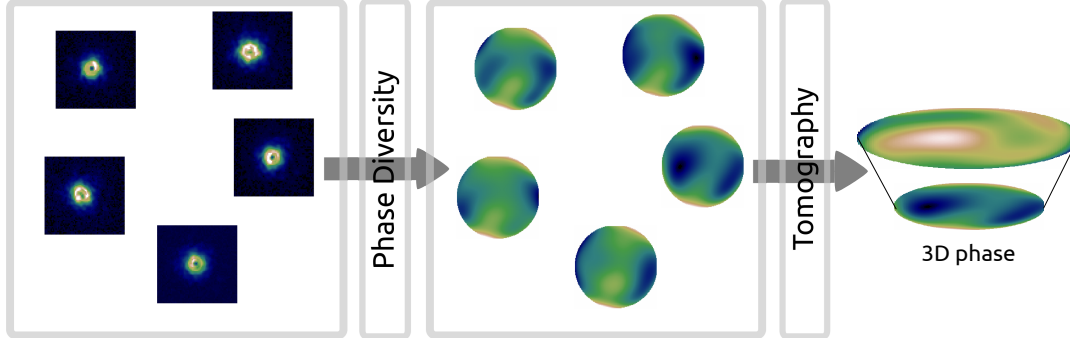
2.3 Non-Common Path Aberrations

In an MCAO system, the correction of the non-common path aberrations (NCPA) follows a slightly different path than for regular, single conjugated AO system. Single-conjugate AO system can only effect static aberration compensation with a single DM, usually pupil conjugated, that will hence be constant across the output field. In contrast, thanks to the multiple-DM 3D phase corrector, MCAO systems have the ability to compensate the NCPA differentially across the output field of view – and correlatively, to degrade them! The goal, for MCAO NCPA, is thus to find the LGS WFS slopes that will produce the best combination of DM actuator commands to simultaneously compensate the PSF static aberrations in the whole output field of view.

To do that, there are several possible methods (see also figure 3):

- The most basic method is just an extension of the "classical" way of doing tomography. This is a two step process:
 - First, the phase is determined in various location of the output focal plane. This can be done with WFS if available (in GeMS, we used a 24x24 SHWFS in the laboratory) or by alternative techniques like phase diversity (e.g. with GSAOI).
 - Second, this set of phases is used as an input to a classical tomography reconstruction, which finally gives phases to apply to the multiple DMs.
- We propose a new approach: tomographic phase diversity. In tomographic phase diversity, all the PSFs are used as an input to the phase diversity minimization process which retrieves directly the multiple-DM phases. This method has several advantages: First, it skips one step, thus is conceptually simpler. Second, it stabilizes the phase diversity process by over-constraining the solution: In the "classical" solution outlined above, N parameters defining the phase are sought for each of the P PSF, so the total number of parameters to find are $N \times P$. In the tomographic phase diversity, the solution only requires $N \times M$ parameters, with M being the number of DMs (typically 2 or 3). In turn, when $P \gg M$, this reduces enormously the number of local minima in the minimization process, and thus provides more faithful solutions that are also more resilient to noise. We implemented successfully this method and were able to reach H band Strehl ratio (static on calibration sources) of 88% averaged over the entire output field (24 PSFs) in two iterations. The tomographic PD process (24 PSFs, 2 output DMs with about 100 modes each) takes about 10 mn on a moderately powerful machine. This algorithm was implemented in two codes: one code, using image-based PD, developed by Damien Gratadour (this code uses analytical derivatives and is significantly faster than the 10mn mentioned above) and one code, using a novel OTF-based PD, developed by François Rigaut. They both give similar results.

Method 1, 2 steps: Phase Diversity + Tomography



Method 2, 1 step: Tomographic Phase Diversity

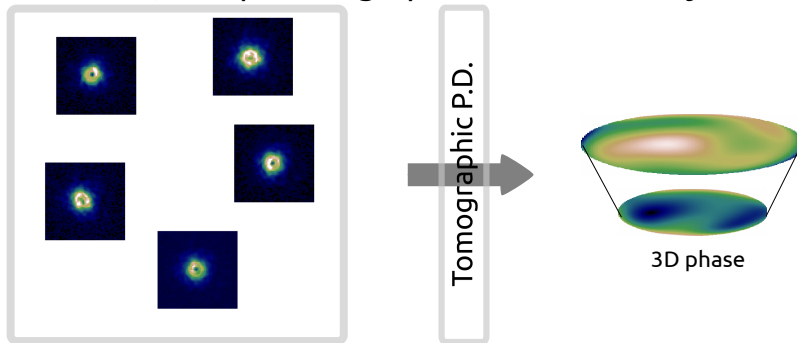


Fig. 3. Non-Common Path Aberrations: Two steps "classical" phase diversity followed by tomography (top), versus one step tomographic phase diversity (bottom).

Some related miscellaneous considerations include:

- If an aberration is induced by an optics which is at an altitude not conjugated to one of the DM, it will generally not be entirely correctable, with the exception of the quadratics (focus and astigmatism). Depending on the instrument, this can be the case of several optics, often conjugated to a very high altitude or even negative altitude.
- Any aberration induced in a single LGS WFS path, if not calibrated out, will reconstruct through the tomographic reconstruction process and induce field variant aberrations. This was initially the case with CANOPUS: within others, there is 600 nm of differential defocus between two of the five LGS WFS. Before being calibrated and subtracted from the slope offsets, this was inducing a field variant astigmatism of up to 500 nm in the corrected images.

2.4 First images

The very first engineering image was acquired with GeMS/GSAOI in April ([5]). This image, obtained in a narrow time window after a crude first focus run and no loop/reconstructor optimization, already showed fairly promising results with FWHM of the order of 75 to 95 mas over a large fraction of the GSAOI field of view.

In December, the GeMS/GSAOI commissioning started the performance optimization phase. The first image was obtained on December 16 on the globular cluster NGC288, and is shown figure 4. All major loops were functional, with the exception of the plate scale and the flexure compensation loops. A focus run was done at the start of acquisition, but the slow focus sensor loop was not used, so focus drifts due to possible variations of the Sodium layer altitude were not compensated. The three TT GS were located in an almost equilateral triangle, well spread and covering most of the GSAOI field of

view. The seeing was $0.7''$ on this night, close to the median seeing for the site. The image (fig4), taken at 1.65 microns (H band) on December 16, 2011, has a field-of-view 87×87 arcseconds. It is a combination of 13 images of 60 seconds each (out of 15 images taken, only 2 were rejected due to poorer-than-average image quality), acquired over the course of 35 minutes. The average full-width at half-maximum is slightly below 0.080 arcsecond, with a variation of 0.002 arcsecond across the entire field of the image. Insets on the right show a detail of the image (top), a comparison –generated from this MCAO corrected image– of the same region with classical AO (middle; this assumes using the star at the upper right corner as the guide star), and seeing-limited observations (bottom). The pixel size in the latter was chosen to optimize the signal-to-noise ratio while not degrading the intrinsic angular resolution of the image². North is up, East is right. The Strehl ratio is relatively low, of the order of 15 to 20%. The relatively large FWHM, compared with what has been obtained more recently, can be explained in part because the plate scale loop was not closed. Nevertheless, the nicely packed PSF, approximately Lorentzian in shape and without marked halo, is extremely uniform across the 87 arcsec field.

A few nights later, during the course of various optimizations, the team gathered news images on the open cluster NGC2362, under good seeing conditions ($< 0.45''$). Figure 5 shows a combination of thirteen 15 seconds images, taken over the course of a 3 hours test. The final image field of view is 85×85 arcsec. Note that these were not dithered, which explains that the gaps between the four arrays³

² Keeping the same pixel size as the MCAO image would have resulted in a lot of noise in the seeing limited image, hence to present a fair comparison, we choose to use larger pixels, also more realistic, to generate the seeing limited image.

³ GSAOI focal plane is populated with four $2k \times 2k$ arrays separated by a gap of about 3 arcsec

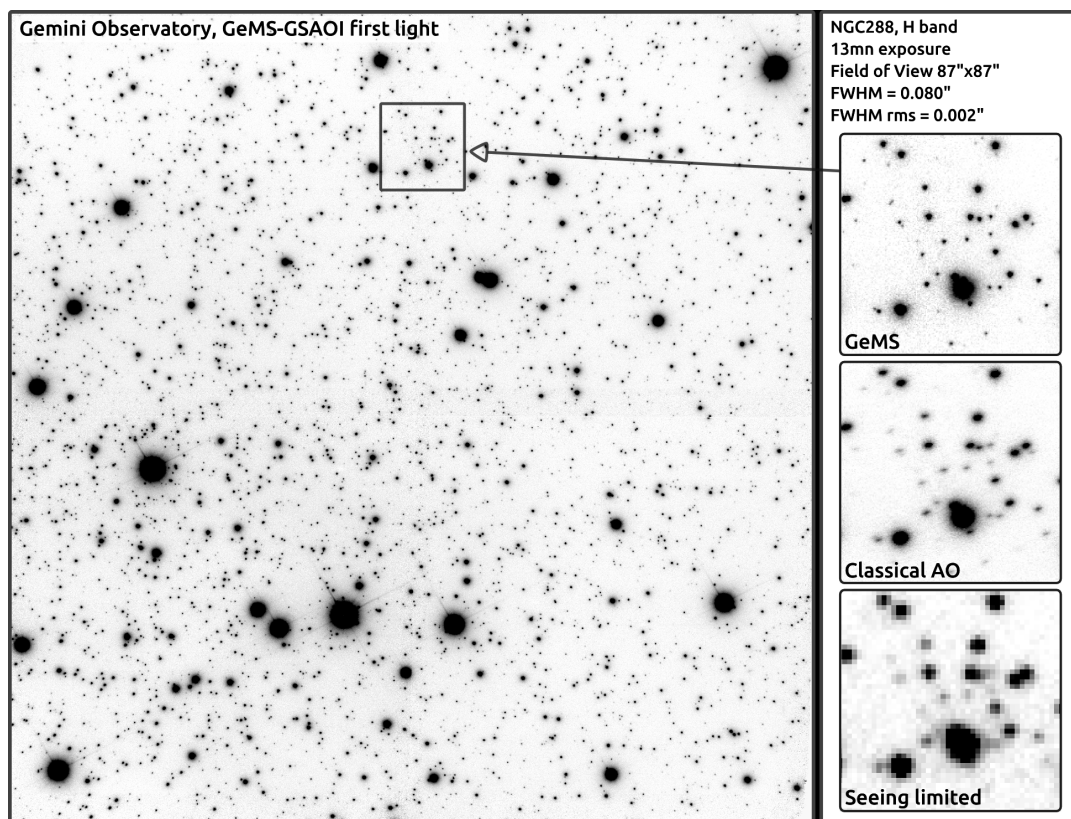


Fig. 4. NGC288 in H band, first light image of GeMS/GSAOI. Exposure time is 13 mn. The field of view is 87×87 arcsec. The FWHM is 80 ± 2 mas.

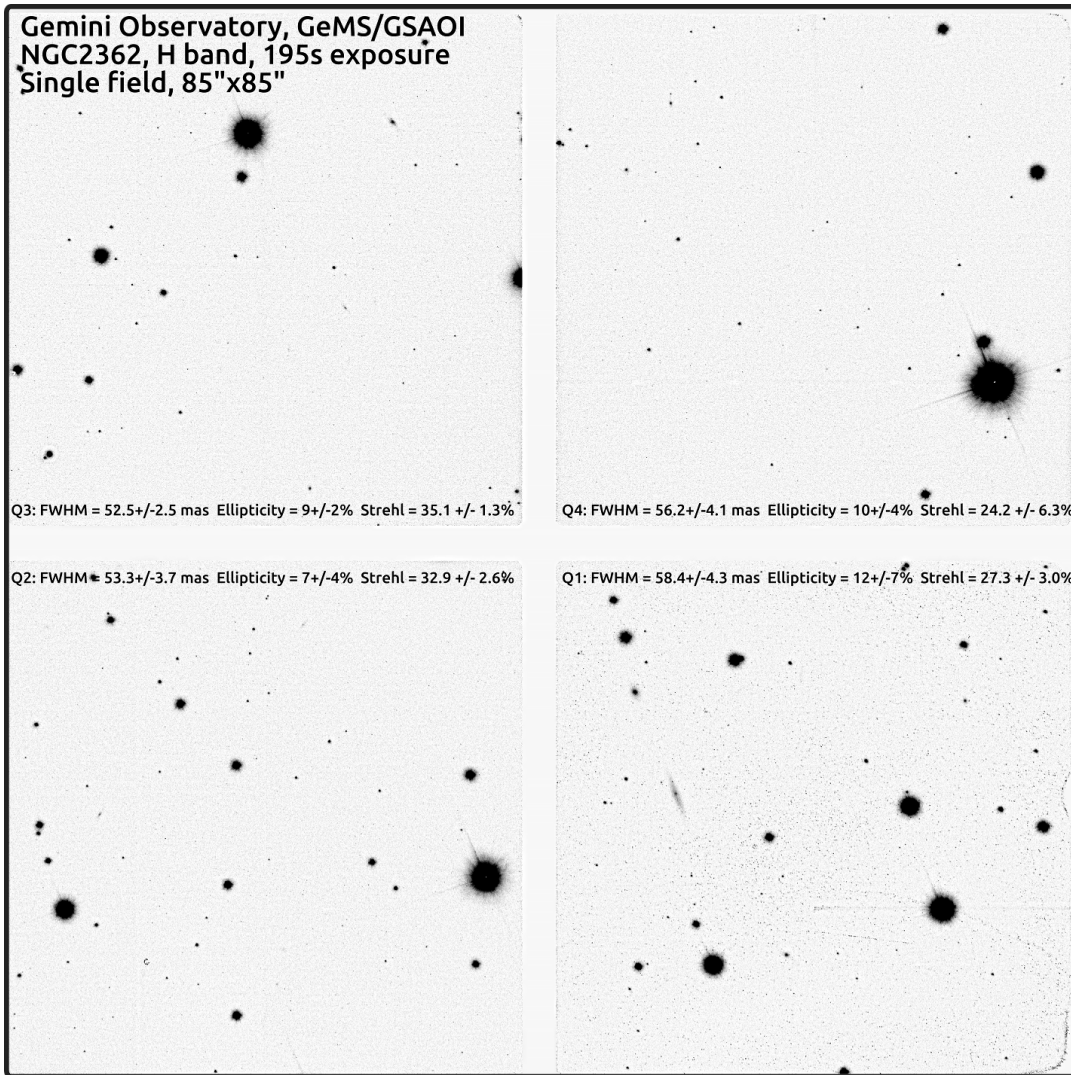


Fig. 5. This H band GeMS/GSAOI image of the open cluster NGC 2362 is a record breaking image. This image is a composite of thirteen 15 seconds images, obtained during GeMS tuning tests during the night of December 18. The average angular resolution on this composite image is about 55 mas, with a Strehl ratio of 30%. Several individual images that served to build this composite had an angular resolution below 50 mas and a Strehl ratio in excess of 40%, which is significantly better than any image obtained with a laser guide star AO system to date. The field of view is 85x85 arc seconds. The white bands between the four GSAOI detectors are the gaps between the arrays, where no signal was collected. North is up, East is right.

is not filled. The three brightest stars were used as TT GS (using the visible TT WFS in CANOPUS). All three fast loops were closed: LGS, TT and plate scale. Again, neither the slow focus nor the flexure compensation loops were closed, not having been commissioned at this time. The FWHM and Strehl numbers, averaged over individual arrays, are reported in the figure. Overall, the performance is rather stable over such a large area for H band AO correction: The lowest array-averaged Strehl is 24%, and the highest 35%. FWHM vary between 52 and 58. Some stars in array 3 (the upper left, noted Q3 in the figure) have Strehl in excess of 40% and FWHM below 50 mas.

Several sets of phase diversity images were acquired on this target along the night and led to residual static aberration estimates equivalent to H band Strehl of 75 to 80%. That would lead to a first pass at the error budget as in the following table:

Source	Strehl	rms error [nm]
TT residuals	0.65	172
High order atmospheric residuals	0.70	157
Static aberrations	0.77	134
Total	0.35	269

The TT residual kernel FWHM was simply derived from a quadratic combination with the diffraction limited kernel, i.e. $\sqrt{(54^2 - 43^2)} = 33$ mas, which –assuming a gaussian distribution– gives a TT rms motion of $33/2.35 = 14$ mas, roughly in line with what was estimated by our on-line Real-Time Display estimator.

This error budget is fairly well balanced. We expect some gains to be possible in the static aberration part (we should be able to reach static Strehl of 85%, as demonstrated without turbulence on calibration sources). The TT error item is on the high side, but assuming the formula $\text{rms}_{\text{noise}} = FWHM / \sqrt{N_{\text{ph}}}$ applies, assuming a noise propagation factor of 1 through the reconstruction and the control loop filtering, and using $FWHM = 0.4$ arcsec, it would correspond to $N_{\text{ph}} \approx 800$ photons, in line with the observed flux. It also can not be excluded that some other sources of error (e.g. imperfect focus through drift of the Sodium layer altitude) was present, in which case it has been wrongly attributed to one of the error term in the above budget. We expect to conduct more systematic measurements in the future to build a better error budget.

Note also that following an issue with one of the internal LGS WFS mechanism, only 4 out of the 5 LGS WFS could be used (the one corresponding to the lower right GSAOI quadrant being the faulty one). Surprisingly, the performance is only marginally degraded in this area.

3 Lessons learned

If we had our current knowledge and were starting all over again, what would we do differently? First of all, it is important to keep this kind of system as simple as possible. One of the drawback of GeMS, is that it combines many very complex sub-systems. Simplicity is key for such, already complex by nature, systems. More specifically, what would we change in GeMS?

- The TT WFS. A design with a focal plane array, using low noise devices as EMCCD or the recent sCMOS would improve dramatically the throughput, alignment complexity and astrometric properties. The current QE of these devices is comparable to APDs, and last but not least, this would made the acquisition much easier, and consequently reduce the overheads. Note as well that the array could be used to obtained visible science images of the targets at the time, information that could be useful for some programs.
- The LGSF. The BTO has to be considered as a full fledge instrument; it is a very complex sub-systems. The required effort and resources have certainly been under-estimated for GeMS, leading to a painful integration and commissioning. Maybe side launch would provide an easier solution?
- Reduce the number of LUTs. When designing the system, many complex aspects are covered by a LUTs. But when times come to commissioning these LUTs, the nightmare begins. Trying to reduce the number of LUTs is important to keep the system at a reasonable complexity level.
- Have a build-in turbulence simulator (e.g. with phase screens). Being able to exercise the AO loops, optimize them, and build a knowledge of the system is key. Having a turbulence simulator could greatly help for this.
- Add a calibration source (focal plane) at the entrance of the LGS WFS path, and keep some degree of freedom in aberration compensation in each non-common path. GeMS deals with 3 non-common path (LGS, NGS and science), being able to keep the best image quality in each of them is challenging. Aberrations in-between the LGS WFS (e.g. differential defocus) would result in non-tomographic errors, and performance lost.

AO4ELT

- Be able to combine LGS and NGS calibration sources simultaneously, and close all loops in the lab, as we do on-sky.
- Move the FSA in a pupil plane, and implement a real-time procedure for the fratricide calibration
- Using quad-cells for the WFS. It adds a non-negligible, even significant complexity due to the need of calibrating the centroid gains.

On the other hand, they are subsystems that we would not change. Examples of those are:

- GSAOI and the ODGW. Having the possibility to read at high rate small region of the science detector is a very powerful tool. One can see immediately what is the effect on the science image to any changes in any parameters (reconstructors, gains, frame rate, focus etc...).
- The optical design of the AO bench. It is fairly simple design, with an easy access, which is important as numerous (always more than expected) optical alignments are required, on the laboratory and even once at the telescope. On top of this, it has proven to be quite robust to vibrations and flexure.
- LGS WFS design & performance (include CCD RON 3.5e-). It has been performing very robustly since the beginning.
- The RTC + Myst (high level software) architecture has provided us with an important (and required) modularity. The diagnostic tools that we have build on this were definitely key during all the commissioning process.
- On the project management side: retaining I&T within the observatory, breaking the whole system into work-packages and a balanced commissioning time and support were very important for the success of GeMS.

4 Conclusion

GeMS is the first instrument of its kind: a Multi-Conjugate adaptive optics system using Laser Guide Stars. It is a very challenging project, combining a lot of complex sub-systems that must work and interact properly together. The first corrected images obtained on-sky demonstrated the potentiality of this instrument. The GeMS commissioning will continue during the first months of 2012, with a focus on the system robustness and the integration into the operational frame of Gemini. First access for the community will be provided in April 2012, with a call for commissioning targets. GeMS will then be in shutdown during the Chilean winter, with a final engineering effort to fix the remaining issues, and it will be eventually offered for Science Verification in 2012B.

The Gemini Observatory is operated by the Association of Universities for Research in Astronomy, Inc., under a cooperative agreement with the NSF on behalf of the Gemini partnership: the National Science Foundation (United States), the Science and Technology Facilities Council (United Kingdom), the National Research Council (Canada), CONICYT (Chile), the Australian Research Council (Australia), Ministerio da Ciencia e Tecnologia (Brazil), and Ministerio de Ciencia, Tecnologia e Innovacion Productiva (Argentina).

References

1. M. Bec et al., Proc. SPIE, Vol. 7015 (2008)
2. F. Rigaut, B. Neichel, M. Bec, M. Boccas, A. Garcia Rissmann & D. Gratadour, AO4ELT, 2009
3. B. Neichel, F. Rigaut, M. Bec & A. Garcia Rissmann, AO4ELT, 2009
4. B. Neichel, F. Rigaut, and M. Bec, M. Boccas, V. Fesquet, C. Dorgeville, & G. Trancho, this conference
5. F. Rigaut, B. Neichel, M. Bec, M. Boccas, C. Dorgeville, V. Fesquet, R. Galvez, G. Gausachs, G. Trancho, C. Trujillo, M. Edwards, R. Carrasco, Proceedings OSA, Toronto 2011
6. D. Gratadour & F. Rigaut, in Adaptive Optics: Analysis and Methods, OSA, paper PMA4 (2007)
7. P. McGregor et al., Proc. SPIE, Vol. 5492 (2004)
8. S. Eikenberry et al., Proc. SPIE, Vol. 7014 (2008)
9. I. Rodriguez, B. Neichel, A. Guesalaga et al., Proceedings OSA, Toronto 2011